

FASTER BINARY EMBEDDINGS FOR PRESERVING EUCLIDEAN DISTANCES

JINJIE ZHANG AND RAYAN SAAB

ABSTRACT. We propose a fast, distance-preserving, binary embedding algorithm to transform a high-dimensional dataset $\mathcal{T} \subseteq \mathbb{R}^n$ into binary sequences in the cube $\{\pm 1\}^m$. When \mathcal{T} consists of well-spread (i.e., non-sparse) vectors, our embedding method applies a stable noise-shaping quantization scheme to Ax where $A \in \mathbb{R}^{m \times n}$ is a sparse Gaussian random matrix. This contrasts with most binary embedding methods, which usually use $x \mapsto \text{sign}(Ax)$ for the embedding. Moreover, we show that Euclidean distances among the elements of \mathcal{T} are approximated by the ℓ_1 norm on the images of $\{\pm 1\}^m$ under a fast linear transformation. This again contrasts with standard methods, where the Hamming distance is used instead. Our method is both fast and memory efficient, with time complexity $O(m)$ and space complexity $O(m)$. Further, we prove that the method is accurate and its associated error is comparable to that of a continuous valued Johnson-Lindenstrauss embedding plus a quantization error that admits a polynomial decay as the embedding dimension m increases. Thus the length of the binary codes required to achieve a desired accuracy is quite small, and we show it can even be compressed further without compromising the accuracy. To illustrate our results, we test the proposed method on natural images and show that it achieves strong performance.

1. INTRODUCTION

Analyzing large data sets of high-dimensional raw data is usually computationally demanding and memory intensive. As a result, it is often necessary – as a preprocessing step – to transform data into a lower-dimensional space while approximately preserving important geometric properties of the data, such as pairwise ℓ_2 distances. As a critical result in dimensionality reduction, the Johnson-Lindenstrauss (JL) lemma [19] guarantees that every finite set $\mathcal{T} \subseteq \mathbb{R}^n$ can be (linearly) mapped to a $m = O(\epsilon^{-2} \log(|\mathcal{T}|))$ dimensional space in such a way that all pairwise distances are preserved up to an ϵ -Lipschitz distortion. Additionally, there are many significant results to either speed up the JL transform by introducing fast embeddings, e.g. [1, 2, 23, 27], or by using sparse matrices [21, 20]. Such fast embeddings can usually be computed in $O(n \log n)$ versus the $O(mn)$ time complexity of JL transforms that rely on unstructured dense matrices.

With the goal of further reducing the memory requirements associated with data processing, in recent years significant progress has been made in *nonlinearly* embedding high-dimensional sets of points $\mathcal{T} \subseteq \mathbb{R}^n$ to the binary cube $\{-1, 1\}^m$ with $m \ll n$, a process known as binary embedding. Specifically, Let \mathcal{T} be a subset of \mathbb{R}^n and $\{-1, 1\}^m$ be the binary cube. Provided that $d_1(\cdot, \cdot)$ is a metric on \mathbb{R}^n , the goal of binary embedding is to find a nonlinear mapping $f : \mathcal{T} \rightarrow \{-1, 1\}^m$ and a function $d_2(\cdot, \cdot)$ on $\{-1, 1\}^m$ such that

$$(1) \quad |d_2(f(x), f(y)) - d_1(x, y)| \leq \alpha, \quad \text{for } \forall x, y \in \mathcal{T}.$$

Due to the potential dimensionality reduction ($m \ll n$) and 1-bit representation per dimension, the storage space used for \mathcal{T} can be considerably reduced and efficient learning and retrieval can happen directly in the binary space using bitwise operations. Most of the existing nonlinear mappings f in (1) are generated by using a simple memory-less scalar quantization (MSQ) technique that nevertheless plays an important role in various applications, including 1-bit compressed sensing [18, 29] and deep neural networks [3]. As an example of such MSQ-based methods, given a set of

unit vectors $\mathcal{T} \subseteq \mathbb{S}^{n-1}$ with finite size $|\mathcal{T}|$, consider the map

$$(2) \quad q_x := f(x) = \text{sign}(Gx)$$

where $G \in \mathbb{R}^{m \times n}$ is a standard Gaussian random matrix and $\text{sign}(\cdot)$ is a binary map which returns the element-wise sign of its argument. Suppose that $d_1(x, y) = \frac{1}{\pi} \arccos(\|x\|_2^{-1} \|y\|_2^{-1} \langle x, y \rangle)$ is the normalized angular distance and $d_2(q_x, q_y) = \frac{1}{2m} \|q_x - q_y\|_1$ is the normalized Hamming distance. Then, as shown in [33], inequality (1) holds with probability at least $1 - \eta$ if $m \gtrsim \alpha^{-2} \log(|\mathcal{T}|/\eta)$, which implies that one can recover the geodesic distance by computing the normalized Hamming distance. This bound on the number of measurements, hence bits, is essentially tight as it is known that any binary embedding method for geodesic distance recovery that is independent of the input data must use $\Omega(\alpha^{-2} \log |\mathcal{T}|)$ bits, see [33]. Although the above random projection G and binary embedding f achieve optimal bit complexity up to constants, it has been observed in practice that the length of the binary sequence m is usually around $O(n)$ to guarantee reasonable accuracy [12, 31, 34]. Moreover, with this construction, since G is dense and unstructured, computing Gx incurs the full computational cost of matrix-vector multiplication, i.e., $O(mn)$. Much like linear Johnson-Lindenstrauss embedding techniques admit fast counterparts, fast binary embedding algorithms have been developed to significantly reduce the computational complexity of binary embeddings (e.g., [14, 25, 13, 12, 24, 30]). More specifically, to reduce the running time and even space complexity, fast Johnson-Lindenstrauss transforms (FJLT) and Gaussian Toeplitz matrices [33], structured hashed projections [4], iterative quantization [14], bilinear projection [12], circulant binary embedding [34, 9, 8, 28, 22], sparse projection [32], and fast orthogonal projection [35] have all been considered.

While these methods can decrease time complexity to $O(n \log n)$ operations per embedding, they still suffer from some important drawbacks. Notably, due to the nature of the sign function, such embedding algorithms completely lose all magnitude information associated with the original dataset \mathcal{T} , as $\text{sign}(Ax) = \text{sign}(A(\alpha x))$ for all $\alpha > 0$. In other words, all points in the same direction will embed to the same binary vector. Moreover, even if one wishes to recover geodesic distances, since using the sign function in (2) is an instance of memoryless scalar quantization, the estimation error α in (1) necessarily decays slowly as the number of bits m increases (e.g., [33]).

More recently [17] resolved these issues by replacing the simple sign function with a Sigma-Delta ($\Sigma\Delta$) quantization scheme, or alternatively other noise-shaping schemes [5]. The distinguishing feature of such quantization methods is their use of memory. They iteratively quantize subsequent coefficients of a vector, based on the quantization results of previous coefficients. These methods are called noise-shaping schemes because in the context of signal recovery (rather than data embedding) the idea is to “shape” the difference between the quantized and unquantized vector so that it is mostly in the kernel of the reconstruction operator. $\Sigma\Delta$ quantization and its relevant properties will be discussed in Section 4. Returning to binary embeddings, [17] use the binary embedding

$$(3) \quad q_x := Q(DBx)$$

where Q is now a stable $\Sigma\Delta$ quantization scheme, $D \in \mathbb{R}^{m \times m}$ is a diagonal matrix with random signs, and $B \in \mathbb{R}^{m \times n}$ is drawn from partial circulant ensemble (PCE) or bounded orthogonal ensemble (BOE) [11, 17]. Put simply, such choices of B allow matrix vector multiplication to be implemented using the fast Fourier transform. Then the original Euclidean distance $\|x - y\|_2$ can be recovered via a pseudo-metric on the quantized vectors given by

$$(4) \quad d_{\tilde{V}}(q_x, q_y) := \|\tilde{V}(q_x - q_y)\|_2$$

where $\tilde{V} \in \mathbb{R}^{p \times m}$ is a “normalized condensation operator”, a sparse matrix that can thus also be applied fast (see Section 4). Importantly, [17] shows that if $m \gtrsim p := \alpha^{-2} \log(|\mathcal{T}|) \log^4 n$ then

$$\left| d_{\tilde{V}}(q_x, q_y) - \|x - y\|_2 \right| \leq c \left(\frac{m}{p} \right)^{-r+1/2} + \alpha \|x - y\|_2,$$

where $c > 0$ is a constant and $r \geq 1$ is the integer order of Q . Regarding the complexity of the construction in [17] applied to a single point $x \in \mathbb{R}^n$, we note that the map $x \mapsto DBx$ has time complexity $O(n \log n)$ while the quantization map needs $O(m)$ time and results in an m bit representation. Thus, when $m \leq n$, the total time complexity for pre-processing (3) is around $O(n \log n)$.

2. CONTRIBUTIONS

In this paper, we propose an extension of these results to the case where DB in (3) is replaced by a sparse Gaussian or sub-Gaussian matrix $A \in \mathbb{R}^{m \times n}$, that is,

$$(5) \quad q_x := Q(Ax).$$

Specifically, given scaled high-dimensional data \mathcal{T} contained in the ℓ_2 ball $B_2^n(\kappa)$ with radius κ , we put forward Algorithm 1 to generate binary sequences and Algorithm 2 to compute estimates of the distances between elements of \mathcal{T} .

Algorithm 1: Fast Binary Embedding for Finite \mathcal{T}

Input: $\mathcal{T} = \{x^{(j)}\}_{j=1}^k \subseteq B_2^n(\kappa)$ ▷ Scaled data points in ℓ_2 ball
1 Generate $A \in \mathbb{R}^{m \times n}$ as in Definition 3.2 ▷ Sparse Gaussian matrix A
2 **for** $j \leftarrow 1$ **to** k **do**
3 $z^{(j)} \leftarrow Ax^{(j)}$
4 $q^{(j)} = Q(z^{(j)})$ ▷ Stable $\Sigma\Delta$ quantizer Q as in (16)
Output: Binary sequences $\mathcal{B} = \{q^{(j)}\}_{j=1}^k \subseteq \{-1, 1\}^m$

Algorithm 2: ℓ_2 Norm Distance Recovery

Input: $q^{(i)}, q^{(j)} \in \mathcal{B}$ ▷ Binary sequences produced by Algorithm 1
1 $y^{(i)} \leftarrow \tilde{V}q^{(i)}$ ▷ Condense the components of q
2 $y^{(j)} \leftarrow \tilde{V}q^{(j)}$
Output: $\|y^{(i)} - y^{(j)}\|_1$ ▷ Approximation of $\|x^{(i)} - x^{(j)}\|_2$

The contribution of this work is threefold.

2.1. Accuracy. We prove Theorem 2.1 quantifying the performance of our algorithms.

Theorem 2.1 (Main result). *Let $\mathcal{T} \subset \mathbb{R}^n$ be a finite set with elements satisfying $\|x\|_\infty = O(n^{-1/2}\|x\|_2)$. If $m \gtrsim p := \epsilon^{-2} \log(|\mathcal{T}|)$ where $c > 0$ is a constant and $r \geq 1$ is the integer order of Q , then with high probability on the draw of the sparse Gaussian matrix A , the following holds uniformly over all x, y in \mathcal{T} : Embedding x, y into $\{-1, 1\}^m$ using Algorithm 1, and estimating the associated distance between them using Algorithm 2 yields the error bound*

$$\left| d_{\tilde{V}}(q_x, q_y) - \|x - y\|_2 \right| \leq c \left(\frac{m}{p} \right)^{-r+1/2} + \epsilon \|x - y\|_2.$$

The significance of such a result is that it yields an approximation error bounded by two components, one due to quantization and another that resembles the error one would obtain from a *linear* Johnson-Lindenstrauss embedding into a p -dimensional space. The latter part behaves like the error in the Johnson-Lindenstrauss lemma and is essentially proportional to $p^{-1/2}$, while the quantization component decays polynomially fast in m , and can thus be rendered harmless by increasing the embedding dimension m . Moreover, the number of bits $m \gtrsim \epsilon^{-2} \log(|\mathcal{T}|)$ achieves the optimal bit complexity required by any oblivious random embedding that preserves Euclidean or squared Euclidean distance, see Theorem 4.1 in [10].

Remark 2.2. Note that Theorem 5.2 is a more precise version of Theorem 2.1, with all quantifiers specified explicitly. In addition, while as stated, Theorem 2.1 applies only to sets with elements satisfying $\|x\|_\infty = O(n^{-1/2}\|x\|_2)$, Theorem 5.2 presents a modification to the matrix A that enables the result to hold for arbitrary finite \mathcal{T} .

2.2. Computational Complexity. By virtue of the sparsity of A , the computation of (5) can be significantly faster than (3), at the expense of having our results restricted to the class of “well-spread” vectors x , i.e., those that are not sparse. On the other hand, in Section 6, we will show that above Algorithm 1 can achieve $O(m)$ time and space complexity in contrast with the common $O(n \log n)$ runtime obtained by the state of the art fast binary embeddings, e.g., [12, 33, 34, 9, 8, 17], which rely on either fast Johnson-Lindenstrauss transforms (FJLT) or circulant matrices. Meanwhile, Algorithm 2 requires only $O(m)$ runtime.

As mentioned in the above remark, if one wants to generalize the results to include arbitrary (including sparse) vectors, one could employ standard techniques (e.g., [1]). Suppose that $H \in \mathbb{R}^{n \times n}$ is the Walsh-Hadamard transform and $D \in \mathbb{R}^{n \times n}$ is a diagonal matrix with random signs, then we can use HD to flatten the input x if necessary, see [1]. Indeed, it suffices to substitute the fast Johnson-Lindenstrauss transform $\Phi = AHD$ (see Definition 3.4) for the sparse matrix A in Algorithm 1. In this case, the time complexity is $O(n \log n)$ again for Algorithm 1.

As an additional advantage that may be relevant to applications, Algorithm 2 only requires the calculation of an ℓ_1 , rather than ℓ_2 norm. If implemented in fixed point arithmetic where each coefficient of $y^{(i)}$ is represented by b bits, the distance computation (a) would not require computations of squares or square-roots, and (b) would require only $b + 1$ bits per embedding dimension to store (rather than $2b$ bits).

2.3. Further Compression. It is also worth mentioning that further reducing the memory footprint of the binary embeddings associated with our methods is easy to accomplish. Indeed, we can see from Definition 3.3 that \tilde{V} is not only sparse, but also essentially populated by integers bounded by $(m/p)^r$ where, r, m, p are as in Theorem 2.1. Thus, each vector $y^{(i)} = \tilde{V}q^{(i)}$ can be represented using $O(p \log(m/p))$ bits, instead of m bits, without affecting the reconstruction accuracy at all.

3. PRELIMINARIES

3.1. Notation and definitions. Throughout this paper, we use $f(n) = O(g(n))$ to denote that $|f(n)|$ is bounded above by a positive function $g(n)$ up to constants asymptotically; that is, $\limsup_{n \rightarrow \infty} \frac{|f(n)|}{g(n)} < \infty$. Similarly, we use $f(n) = \Theta(g(n))$ to denote that $f(n)$ is bounded both above and below by a positive function $g(n)$ up to constants asymptotically.

We next define operator norms.

Definition 3.1. Let $\alpha, \beta \in [1, \infty]$ be integers. The (α, β) operator norm of a matrix $K \in \mathbb{R}^{m \times n}$ is defined by

$$\|K\|_{\alpha, \beta} = \max_{x \neq 0} \frac{\|Kx\|_\beta}{\|x\|_\alpha}.$$

We now introduce some notation and definitions that are relevant to our construction.

Definition 3.2 (Sparse Gaussian random matrix). Let $A = (a_{ij}) \in \mathbb{R}^{m \times n}$ be a random matrix with i.i.d. entries such that a_{ij} takes value 0 with probability $1 - s$ and a value drawn from $\mathcal{N}(0, \frac{1}{s})$ with probability s .

Indeed, we can construct a_{ij} by $a_{ij} = b_{ij}c_{ij}$ where $b_{ij} \sim \text{Bernoulli}(s)$, $c_{ij} \sim \mathcal{N}(0, \frac{1}{s})$ and all b_{ij} and c_{ij} are independent. Moreover, $\mathbb{E}(a_{ij}) = 0$ and $\text{Var}(a_{ij}) = 1$ for all $1 \leq i \leq m$ and $1 \leq j \leq n$. We adopt the definition of a condensation operator in [17] (see also [5]).

Definition 3.3 (Condensation operator). Let p, r, λ be fixed positive integers such that $\lambda = r\tilde{\lambda} - r + 1$ for some integer $\tilde{\lambda}$. Let $m = \lambda p$ and v be a row vector in \mathbb{R}^λ whose entry v_j is the j -th coefficient of the polynomial $(1 + z + \dots + z^{\tilde{\lambda}-1})^r$. Define the condensation operator $V \in \mathbb{R}^{p \times m}$ by

$$V = I_p \otimes v = \begin{bmatrix} v & & & \\ & v & & \\ & & \ddots & \\ & & & v \end{bmatrix}.$$

For example, when $r = 1$, $\lambda = \tilde{\lambda}$, and the vector $v \in \mathbb{R}^\lambda$ is simply the vector of all ones. The normalized condensation operator is given by

$$\tilde{V} = \frac{\sqrt{\pi/2}}{p\|v\|_2} V.$$

The fast Johnson-Lindenstrauss transform (FJLT) was first studied by Ailon and Chazelle [1]. It admits many variants and improved versions (e.g., [23, 26]). The idea is that given any high dimensional data point $x \in \mathbb{R}^n$ we use a bounded orthonormal ensemble (BOE) that admits a fast transform, as the Walsh-Hadamard transform does, to distribute the total mass (i.e. $\|x\|_2$) of x relatively evenly to its coordinates. So when we multiply a sparse Gaussian matrix A by a well spread vector \tilde{x} , one can expect that $\|A\tilde{x}\|_1$ is concentrated as needed.

Definition 3.4 (FJLT). The fast Johnson-Lindenstrauss transform can be obtained by

$$(6) \quad \Phi := AHD \in \mathbb{R}^{m \times n}.$$

Here, $A \in \mathbb{R}^{m \times n}$ is a sparse Gaussian random matrix, as in Definition 3.2, while $H \in \mathbb{R}^{n \times n}$ is a normalized Walsh-Hadamard matrix defined by

$$H_{ij} = n^{-1/2}(-1)^{\langle i, j \rangle}$$

where $\langle i, j \rangle$ is the bitwise dot product of the binary representations of the numbers i and j . Finally, $D \in \mathbb{R}^{n \times n}$ is simply a diagonal matrix with diagonal entries drawn independently from $\{-1, 1\}$ with probability $1/2$ for each of -1 and 1 .

3.2. Preliminary lemmata. We will require the following lemmas, adapted from the literature, to prove the distance-preserving properties of our condensed sparse Johnson-Lindenstrauss transform (CSJLT) and condensed fast Johnson-Lindenstrauss transform (CFJLT) in Lemma 3.7.

Lemma 3.5 (Theorem 5.1 in [26]). *Let $n \in \mathbb{N}$, $\epsilon \in (0, \frac{1}{2})$, $\delta \in (0, 1)$, $\alpha \in [\frac{1}{\sqrt{n}}, 1]$ be parameters and set $m = C\epsilon^{-2} \log(\delta^{-1}) \in \mathbb{N}$ where C is a sufficiently large constant. Let $s = 2\alpha^2/\epsilon \leq 1$, $A \in \mathbb{R}^{m \times n}$ be as in Definition 3.2. Then*

$$(7) \quad \mathbb{P}\left((1 - \epsilon)\|x\|_2 \leq \frac{\sqrt{\pi/2}}{m}\|Ax\|_1 \leq (1 + \epsilon)\|x\|_2\right) \geq 1 - \delta$$

holds for all $x \in \mathbb{R}^n$ with $\|x\|_\infty \leq \alpha\|x\|_2$.

Lemma 3.6 below is adapted from [1, Lemma 1], and we present its proof for completeness.

Lemma 3.6. *Let $H \in \mathbb{R}^{n \times n}$ and $D \in \mathbb{R}^{n \times n}$ be as in Definition 3.4. For any $\lambda > 0$ and $x \in \mathbb{R}^n$ we have*

$$(8) \quad \mathbb{P}\left(\|HDx\|_\infty \leq \lambda\|x\|_2\right) \geq 1 - 2ne^{-n\lambda^2/2}.$$

Proof. Without loss of generality, we can assume $\|x\|_2 = 1$. Let $u = HDx = (u_1, \dots, u_n)$. Fix $i \in \{1, \dots, n\}$. Then $u_i = \sum_{j=1}^n a_j x_j$ with $\mathbb{P}\left(a_j = \frac{1}{\sqrt{n}}\right) = \mathbb{P}\left(a_j = -\frac{1}{\sqrt{n}}\right) = \frac{1}{2}$ for all j . Moreover,

a_1, a_2, \dots, a_n are independent and symmetric. So u_i is also symmetric, that is, u_i and $-u_i$ share the same distribution. For any $t \in \mathbb{R}$ we have

$$\mathbb{E}(e^{tnu_i}) = \prod_{j=1}^n \mathbb{E}[\exp(tna_j x_j)] = \prod_{j=1}^n \frac{\exp(t\sqrt{n}x_j) + \exp(-t\sqrt{n}x_j)}{2} \leq \prod_{j=1}^n \exp(nt^2 x_j^2 / 2) = \exp(nt^2 / 2).$$

Since u_i is symmetric, by Markov's inequality and the above result, we get

$$\mathbb{P}(|u_i| \geq \lambda) = 2\mathbb{P}(e^{\lambda n u_i} \geq e^{\lambda^2 n}) \leq 2e^{-\lambda^2 n} \mathbb{E}(e^{\lambda n u_i}) = 2e^{-\lambda^2 n / 2}.$$

Inequality (8) follows by the union bound over all $i \in \{1, \dots, n\}$. \square

Now we will prove the condensed Johnson-Lindenstrauss transform (CJLT) lemma whose main purpose is to show that the action of the condensation operator on \tilde{V} on A , does not harm the distance preserving properties of A .

Theorem 3.7 (CJLT lemma). *Let $n, \lambda \in \mathbb{N}$, $\epsilon \in (0, \frac{1}{2})$, $\delta \in (0, 1)$, $p = O(\epsilon^{-2} \log(\delta^{-1})) \in \mathbb{N}$ and $m = \lambda p$. Let $\tilde{V} \in \mathbb{R}^{p \times m}$ and $\Phi = AHD \in \mathbb{R}^{m \times n}$ be as in Definition 3.3 and Definition 3.4 respectively with $s = \Theta(\epsilon^{-1} n^{-1} (\|v\|_\infty / \|v\|_2)^2) \leq 1$. Then for $x \in \mathbb{R}^n$ with $\|x\|_\infty = O(n^{-1/2} \|x\|_2)$, we have*

$$(9) \quad \mathbb{P}\left((1 - \epsilon)\|x\|_2 \leq \|\tilde{V}Ax\|_1 \leq (1 + \epsilon)\|x\|_2\right) \geq 1 - \delta,$$

and for arbitrary $x \in \mathbb{R}^n$, we have

$$(10) \quad \mathbb{P}\left((1 - \epsilon)\|x\|_2 \leq \|\tilde{V}\Phi x\|_1 \leq (1 + \epsilon)\|x\|_2\right) \geq 1 - \delta.$$

Proof. Recall that $V = I_p \otimes v$ and $\Phi = AHD$. Let $y \in \mathbb{R}^n$ and $K := VA = (I_p \otimes v)A \in \mathbb{R}^{p \times n}$. For $1 \leq i \leq p$ and $1 \leq j \leq n$, we have

$$K_{ij} = \sum_{k=1}^{\lambda} v_k a_{(i-1)\lambda+k, j}.$$

Denote the row vectors of A by a_1, a_2, \dots, a_m . It follows that

$$(Ky)_i = \sum_{j=1}^n K_{ij} y_j = \sum_{j=1}^n \sum_{k=1}^{\lambda} y_j v_k a_{(i-1)\lambda+k, j} = \sum_{k=1}^{\lambda} v_k \langle y, a_{(i-1)\lambda+k} \rangle = [B(v^\top \otimes y)]_i$$

where

$$B := \begin{bmatrix} a_1 & a_2 & \dots & a_\lambda \\ a_{\lambda+1} & a_{\lambda+2} & \dots & a_{2\lambda} \\ \vdots & \vdots & & \vdots \\ a_{(p-1)\lambda+1} & a_{(p-1)\lambda+2} & \dots & a_{p\lambda} \end{bmatrix} \in \mathbb{R}^{p \times \lambda n} \quad \text{and} \quad v^\top \otimes y = \begin{bmatrix} v_1 y \\ v_2 y \\ \vdots \\ v_\lambda y \end{bmatrix} \in \mathbb{R}^{\lambda n}.$$

Hence $VAy = Ky = B(v^\top \otimes y)$ holds for all $y \in \mathbb{R}^n$. Additionally, we get a reshaped sparse Gaussian random matrix B by rearranging the rows of A .

For the first assertion in the theorem, note that $x \in \mathbb{R}^n$ satisfies $\|x\|_\infty = O(\|x\|_2 / \sqrt{n})$. So, we have $VAx = B(v^\top \otimes x)$, $\|v^\top \otimes x\|_2 = \|v\|_2 \|x\|_2$ and $\|v^\top \otimes x\|_\infty = \|v\|_\infty \|x\|_\infty$. Then (9) holds by applying Lemma 3.5 to random matrix B and vector $v^\top \otimes x$ with $\alpha = \Theta(n^{-1/2} \|v\|_\infty / \|v\|_2)$.

For the second assertion, if $x \in \mathbb{R}^n$ is arbitrary, then by substituting HDx for y one can get

$$V\Phi x = B(v^\top \otimes (HDx)).$$

Note that

$$\|v^\top \otimes (HDx)\|_2 = \|v\|_2 \|HDx\|_2 = \|v\|_2 \|x\|_2 \quad \text{and} \quad \|v^\top \otimes (HDx)\|_\infty = \|v\|_\infty \|HDx\|_\infty.$$

Inequality (10) follows immediately by using above fact and applying Lemma 3.5 and Lemma 3.6 to the random operator B and vector $v^\top \otimes (HDx)$ with $\alpha = \Theta(n^{-1/2}\|v\|_\infty/\|v\|_2)$. \square

Now we can embed a set of points in a high dimensional space into a space of much lower dimension in such a way that distances between the points are nearly preserved. By substituting δ with $2\delta/|\mathcal{T}|^2$ in Theorem 3.7 and using the fact $1 - \binom{|\mathcal{T}|}{2} \frac{2\delta}{|\mathcal{T}|^2} = 1 - \frac{|\mathcal{T}|(|\mathcal{T}|-1)}{2} \cdot \frac{2\delta}{|\mathcal{T}|^2} > 1 - \delta$, Corollary 3.8 follows from the union bound over all pairwise data points in \mathcal{T} .

Corollary 3.8. *Let \mathcal{T} be a finite subset of \mathbb{R}^n , $\lambda \in \mathbb{N}$, $\epsilon \in (0, \frac{1}{2})$, $\delta \in (0, 1)$, $p = O(\epsilon^{-2} \log(|\mathcal{T}|^2/\delta)) \in \mathbb{N}$ and $m = \lambda p$. Let $\tilde{V} \in \mathbb{R}^{p \times m}$ and $\Phi = AHD \in \mathbb{R}^{m \times n}$ be as in Definition 3.3 and Definition 3.4 respectively with $s = \Theta(\epsilon^{-1} n^{-1} (\|v\|_\infty/\|v\|_2)^2) \leq 1$. If \mathcal{T} consists of well-spread vectors, that is, $\|x\|_\infty = O(n^{-1/2}\|x\|_2)$ for all $x \in \mathcal{T}$, then*

$$(11) \quad \left| \|\tilde{V}A(x-y)\|_1 - \|x-y\|_2 \right| \leq \epsilon \|x-y\|_2$$

holds uniformly for all $x, y \in \mathcal{T}$ with probability at least $1 - \delta$. Moreover, if \mathcal{T} contains arbitrary vectors in \mathbb{R}^n , then

$$(12) \quad \left| \|\tilde{V}\Phi(x-y)\|_1 - \|x-y\|_2 \right| \leq \epsilon \|x-y\|_2$$

holds uniformly for all $x, y \in \mathcal{T}$ with probability at least $1 - \delta$.

Our condensed sparse Johnson-Lindenstrauss transform (CSJLT) is given by $\tilde{V}A$, while the condensed fast Johnson-Lindenstrauss transform (CFJLT) is a composition of two linear operators \tilde{V} and $\Phi = AHD$, in which (sparse) random matrices $A, \Phi \in \mathbb{R}^{m \times n}$ are used to reduce the dimension of the data in a way that preserves its relevant structure and $\tilde{V} \in \mathbb{R}^{p \times m}$ condenses the transformed data to guarantee reconstruction accuracy by $\Sigma\Delta$ quantization discussed latter. So the original finite data set $\mathcal{T} \subseteq \mathbb{R}^n$ is embedded into \mathbb{R}^p with pairwise distances distorted at most ϵ , where $p = O(\epsilon^{-2} \log |\mathcal{T}|)$ as one would expect from a JL embedding. Note that above dimension p does not require extra logarithmic factors containing $|\mathcal{T}|$ or n in contrast to the embedding dimension $O(\epsilon^{-2} \log |\mathcal{T}| \log^4 n)$ in [17].

4. SIGMA-DELTA QUANTIZATION

An r -th order $\Sigma\Delta$ quantizer $Q^{(r)} : \mathbb{R}^m \rightarrow \mathcal{A}^m$ maps an input signal $y = (y_i)_{i=1}^m \in \mathbb{R}^m$ to a quantized sequence $q = (q_i)_{i=1}^m \in \mathcal{A}^m$ via a quantization rule ρ and the following iterations

$$(13) \quad \begin{cases} u_0 = u_{-1} = \dots = u_{1-r} = 0, \\ q_i = Q(\rho(y_i, u_{i-1}, \dots, u_{i-r})) \quad \text{for } i = 1, 2, \dots, m, \\ P^r u = y - q \end{cases}$$

where $Q(y) = \operatorname{argmin}_{v \in \mathcal{A}} |y - v|$ is the scalar quantizer related to alphabet \mathcal{A} and $P \in \mathbb{R}^{m \times m}$ is the first order difference matrix defined by

$$P_{ij} = \begin{cases} 1 & \text{if } i = j, \\ -1 & \text{if } i = j + 1, \\ 0 & \text{otherwise.} \end{cases}$$

While (13) may appear to be not amenable to an iterative update of the state variables u_i , in fact it is, as the difference equation

$$(14) \quad P^r u = y - q$$

can be rewritten as

$$u_i = \sum_{j=1}^r (-1)^{j-1} \binom{r}{j} u_{i-j} + y_i - q_i, \quad i = 1, 2, \dots, m.$$

Definition 4.1. A quantization scheme is called *stable* if there exists $\mu > 0$ such that for each bounded input signal with $\|y\|_\infty \leq \mu$, the state vector $u \in \mathbb{R}^m$ satisfies $\|u\|_\infty \leq C$. Here, crucially, the constants μ and C do not depend on m .

Note that stability heavily depends on the choice of quantization rule and it is difficult to guarantee for arbitrary functions ρ in (13), particularly when one works with a small alphabet as one does in the case of 1-bit quantization corresponding to $\mathcal{A} = \{\pm 1\}$.

When $r = 1$ and the alphabet $\mathcal{A} = \{\pm 1\}$, the simplest stable $\Sigma\Delta$ scheme $Q^{(1)} : \mathbb{R}^m \rightarrow \mathcal{A}^m$ is equipped with the greedy quantization rule $\rho(y_i, u_{i-1}) := u_{i-1} + y_i$ giving the simple iteration

$$\begin{cases} u_0 = 0, \\ q_i = \text{sign}(u_{i-1} + y_i), \\ u_i = u_{i-1} + y_i - q_i, \end{cases}$$

for $i = 1, 2, \dots, m$.

Although it is a non-trivial task to design a stable quantization rule ρ when $r > 1$, families of one-bit $\Sigma\Delta$ quantization schemes that achieve this goal have been designed [6, 15, 7], and we now describe one such family. To start, note that an r -th order $\Sigma\Delta$ quantization scheme may also arise from a more general difference equation of the form

$$(15) \quad y - q = f * v$$

where $*$ denotes convolution and the sequence $f = P^r g$ with $g \in \ell^1$. Then any (bounded) solution v of (15) generates a (bounded) solution u of (14) via $u = g * v$. Thus (14) can be rewritten in the form (15) by a change of variables. Defining $h := \delta^{(0)} - f$, where $\delta^{(0)}$ denotes the Kronecker delta sequence supported at 0, and choosing the quantization rule ρ in terms of the new variable as $(h * v)_i + y_i$. Then (13) reads as

$$(16) \quad \begin{cases} q_i = Q((h * v)_i + y_i), \\ v_i = (h * v)_i + y_i - q_i. \end{cases}$$

By designing a proper filter h one can get a stable r -th order $\Sigma\Delta$ quantizer, as was done in [7, 15], leading to the following result from [15], which exploits the above relationship between v and u to bound $\|u\|_\infty$.

Proposition 4.2. Fix an integer r , an integer $\sigma \geq 6$ and let $n_j = \sigma(j-1)^2 + 1$ for $j = 1, 2, \dots, r$. Let the filter h be of the form

$$h = \sum_{j=1}^r d_j \delta^{n_j}$$

where δ^{n_j} is the Kronecker delta supported at n_j and $d_j = \prod_{i \neq j} \frac{n_i}{n_i - n_j}$ for $j = 1, 2, \dots, r$. There exists a universal constant $C > 0$ such that the r th order $\Sigma\Delta$ scheme (16) with 1-bit alphabet $\mathcal{A} = \{-1, 1\}$, is stable, and

$$(17) \quad \|y\|_\infty \leq \mu < 1 \implies \|u\|_\infty \leq Cc(\mu)^r r^r,$$

where $c(\mu) > 0$ is a constant only depends on μ .

Having introduced stable $\Sigma\Delta$ quantization, we now present a lemma controlling an operator norm of $\tilde{V}P^r$. We will need this result in controlling the error in approximating distances associated with our binary embedding.

Lemma 4.3. *For a stable r -th order $\Sigma\Delta$ quantization scheme,*

$$\|\tilde{V}P^r\|_{\infty,1} \leq \sqrt{\pi/2}(8r)^{r+1}\lambda^{-r+1/2}.$$

Proof. By the same method used in the proof of Lemma 4.6 in [17], one can get

$$\|VP^r\|_{\infty,\infty} \leq r2^{3r-1} \quad \text{and} \quad \|v\|_2 \geq \lambda^{r-1/2}r^{-r}.$$

It follows that

$$\|\tilde{V}P^r\|_{\infty,1} = \frac{\sqrt{\pi/2}}{p\|v\|_2}\|VP^r\|_{\infty,1} \leq \frac{\sqrt{\pi/2}}{\|v\|_2}\|VP^r\|_{\infty,\infty} \leq \sqrt{\pi/2}(8r)^{r+1}\lambda^{-r+1/2}.$$

□

The following result guarantees that the linear part of our embedding generates a bounded vector, and therefore allows us to later appeal to the stability property of $\Sigma\Delta$ quantizers. In other words, it will allow us to use (17) to control the infinity norm of state vectors generated by $\Sigma\Delta$ quantization.

Lemma 4.4 (Concentration inequality for $\|\cdot\|_\infty$). *Let $\beta > 0$, $\epsilon \in (0, 1)$ and $\Phi = AHD \in \mathbb{R}^{m \times n}$ be the FJLT in Definition 3.4 with $s = \Theta(\epsilon^{-1}n^{-1}) \leq 1$. If*

$$(18) \quad 2\sqrt{\beta + \log(2m)} \leq \mu \leq \frac{4}{\sqrt{\epsilon}},$$

then

$$(19) \quad \mathbb{P}(\|Ax\|_\infty \leq \mu\|x\|_2) \geq 1 - e^{-\beta}$$

holds for $x \in \mathbb{R}^n$ with $\|x\|_\infty = O(n^{-1/2}\|x\|_2)$ and

$$(20) \quad \mathbb{P}(\|\Phi x\|_\infty \leq \mu\|x\|_2) \geq 1 - 2e^{-\beta}$$

holds for $x \in \mathbb{R}^n$.

Proof. Without loss of generality, we can assume that x is a unit vector with $\|x\|_2 = 1$. By applying Lemma 3.6 to x with $\lambda = \Theta(n^{-1/2})$, we have

$$(21) \quad \mathbb{P}(\|HDx\|_\infty \leq \lambda) \geq 1 - e^{-\beta}.$$

Let A be as in Definition 3.2 with $s = 2\lambda^2/\epsilon = \Theta(\epsilon^{-1}n^{-1}) \leq 1$ and recall that $\Phi = AHD$.

Suppose that $y \in \mathbb{R}^n$ with $\|y\|_2 = 1$ and $\|y\|_\infty \leq \lambda$. Let $Y = Ay$. Then $Y_i := (Ay)_i = \sum_{j=1}^n a_{ij}y_j$ for $1 \leq i \leq m$. For $t \leq t_0 := \sqrt{2s}/\lambda = 2/\sqrt{\epsilon}$, we get $t^2y_j^2/2s \leq 1$ for all j . Since $e^x \leq 1 + 2x$ for all $x \in [0, 1]$ and $1 + x \leq e^x$ for all $x \in \mathbb{R}$, $se^{t^2y_j^2/2s} + 1 - s \leq s(1 + t^2y_j^2/s) + 1 - s = 1 + t^2y_j^2 \leq e^{t^2y_j^2}$. It follows that

$$\mathbb{E}(e^{tY_i}) = \prod_{j=1}^n \mathbb{E}(e^{ta_{ij}y_j}) = \prod_{j=1}^n (se^{t^2y_j^2/2s} + 1 - s) \leq \prod_{j=1}^n e^{t^2y_j^2} = e^{t^2}$$

holds for all $1 \leq i \leq m$ and $t \in [0, t_0]$. So for $t \in [0, t_0]$, by Markov inequality and above inequality we have

$$\mathbb{P}(Y_i \geq \mu) = \mathbb{P}(e^{tY_i} \geq e^{t\mu}) \leq e^{-t\mu}\mathbb{E}(e^{tY_i}) \leq e^{-t\mu+t^2}.$$

According to (18) we can set $t = \mu/2 \leq t_0 = 2/\sqrt{\epsilon}$, then $\mathbb{P}(Y_i \geq \mu) \leq e^{-\mu^2/4}$. By symmetry we have $\mathbb{P}(-Y_i \geq \mu) \leq e^{-\mu^2/4}$. Consequently, for all $1 \leq i \leq m$ we have

$$(22) \quad \mathbb{P}(|Y_i| \geq \mu) \leq 2e^{-\mu^2/4}.$$

By a union bound, (18), and (22)

$$(23) \quad \begin{aligned} \mathbb{P}(\|Ay\|_\infty \geq \mu) &= \mathbb{P}\left(\max_{1 \leq i \leq m} |Y_i| \geq \mu\right) \leq m\mathbb{P}\left(|Y_i| \geq \mu\right) \\ &= 2me^{-\mu^2/4} \leq e^{-\beta}. \end{aligned}$$

It follows immediately from (21) and (23) with $y = HDx$ that

$$\begin{aligned} \mathbb{P}(\|\Phi x\|_\infty \leq \mu) &= \mathbb{P}(\|AHDx\|_\infty \leq \mu) \\ &\geq \mathbb{P}(\|AHDx\|_\infty \leq \mu, \|HDx\|_\infty \leq \lambda) \\ &= \mathbb{P}(\|AHDx\|_\infty \leq \mu \mid \|HDx\|_\infty \leq \lambda)\mathbb{P}(\|HDx\|_\infty \leq \lambda) \\ &\geq (1 - e^{-\beta})^2 \\ &\geq 1 - 2e^{-\beta}. \end{aligned}$$

Furthermore, if we replace y by x in (23), then inequality (19) follows. \square

5. MAIN RESULTS

As mentioned previously, the ingredients that make our construction work are a Johnson-Lindenstrauss embedding followed by $\Sigma\Delta$ quantization. Together these embed points into the cube $\{\pm 1\}^m$, but it remains to define a pseudometric so that we may approximate Euclidean distances by distances on the cube. We now define this pseudometric.

Definition 5.1. Let $\mathcal{A}^m = \{-1, 1\}^m$ be the discrete cube in \mathbb{R}^m and let $V \in \mathbb{R}^{p \times m}$ with $p \leq m$. We can define a pseudometric d_V on \mathcal{A}^m as

$$d_V(q_1, q_2) = \|V(q_1 - q_2)\|_1 \quad \forall q_1, q_2 \in \mathcal{A}^m.$$

We are now ready to present our main result guaranteeing that our method works and produces a quantization error that decays polynomially in m .

Theorem 5.2 (Main result). *Let $\lambda, r \in \mathbb{N}$, $\epsilon \in (0, \frac{1}{2})$, $\delta \in (0, 1)$, $\mu \in (0, 1)$, $\beta > 0$, $p = O(\epsilon^{-2} \log(|\mathcal{T}|^2/\delta)) \in \mathbb{N}$ and $m = \lambda p$. Moreover, let $\tilde{V} \in \mathbb{R}^{p \times m}$ and $\Phi = AHD \in \mathbb{R}^{m \times n}$ be as in Definition 3.3 and Definition 3.4 respectively with $s = \Theta(\epsilon^{-1} n^{-1} (\|v\|_\infty / \|v\|_2)^2) \leq 1$.*

Let \mathcal{T} be a finite subset of $B_2^n(\kappa) := \{x \in \mathbb{R}^n : \|x\|_2 \leq \kappa\}$ and suppose that

$$\kappa \leq \frac{\mu}{2\sqrt{\beta + \log(2m)}}.$$

Defining the embedding maps $f_1 : \mathcal{T} \rightarrow \{\pm 1\}^m$ by $f_1 = Q^{(r)} \circ A$ and $f_2 : \mathcal{T} \rightarrow \{\pm 1\}^m$ by $f_2 = Q^{(r)} \circ \Phi$, there exists a constant $C(\mu, r)$ which depends on μ and r such that the following are true:

(i) *If the elements of \mathcal{T} satisfy $\|x\|_\infty = O(n^{-1/2}\|x\|_2)$, then*

$$(24) \quad \left| d_{\tilde{V}}(f_1(x), f_1(y)) - \|x - y\|_2 \right| \leq C(\mu, r)\lambda^{-r+1/2} + \epsilon\|x - y\|_2$$

holds uniformly for all $x, y \in \mathcal{T}$ with probability exceeding $1 - \delta - |\mathcal{T}|e^{-\beta}$.

(ii) *On the other hand, for arbitrary $\mathcal{T} \subset B_2^n(\kappa)$*

$$(25) \quad \left| d_{\tilde{V}}(f_2(x), f_2(y)) - \|x - y\|_2 \right| \leq C(\mu, r)\lambda^{-r+1/2} + \epsilon\|x - y\|_2$$

holds uniformly for any $x, y \in \mathcal{T}$ with probability exceeding $1 - \delta - 2|\mathcal{T}|e^{-\beta}$.

Proof. Since the proofs of (24) and (25) are almost identical except for using different random projections A and Φ , we shall only establish the result for (25) in detail. For any $x \in \mathcal{T} \subseteq B_2^n(\kappa)$ we have $\|x\|_2 \leq \kappa$. By applying Lemma 4.4 we get

$$\mathbb{P}(\|\Phi x\|_\infty < \mu) \geq \mathbb{P}(\|\Phi x\|_\infty < \mu\|x\|_2/\kappa) \geq \mathbb{P}(\|\Phi x\|_\infty < 2\sqrt{\beta + \log(2m)}\|x\|_2) \geq 1 - 2e^{-\beta}.$$

Since above inequality holds for arbitrary $x \in \mathcal{T}$, by union bound one can get

$$\mathbb{P}\left(\max_{x \in \mathcal{T}} \|\Phi x\|_\infty < \mu\right) \geq 1 - 2|\mathcal{T}|e^{-\beta}.$$

Suppose that u_x is the state vector of input signal Φx which is produced by stable r -th order $\Sigma\Delta$ scheme. Using Lemma 4.3 and formula (17) to get

$$(26) \quad \|\tilde{V}P^r\|_{\infty,1}\|u_x\|_\infty \leq Cc(\mu)^r r^r (8r)^{r+1} \sqrt{\pi/2} \lambda^{-r+1/2},$$

which holds uniformly for all $x \in \mathcal{T}$ with probability exceeding $1 - 2|\mathcal{T}|e^{-\beta}$.

Furthermore, by Corollary 3.8 the probability that

$$(27) \quad \left| \|\tilde{V}\Phi(x-y)\|_1 - \|x-y\|_2 \right| \leq \epsilon \|x-y\|_2.$$

holds simultaneously for all $x, y \in \mathcal{T}$ is at least $1 - \delta$.

We deduce from triangle inequality and equations (26), (27) that

$$\begin{aligned} \left| d_{\tilde{V}}(f_2(x), f_2(y)) - \|x-y\|_2 \right| &= \left| \|\tilde{V}Q^{(r)}(\Phi x) - \tilde{V}Q^{(r)}(\Phi y)\|_1 - \|x-y\|_2 \right| \\ &\leq \left| \|\tilde{V}Q^{(r)}(\Phi x) - \tilde{V}Q^{(r)}(\Phi y)\|_1 - \|\tilde{V}\Phi(x-y)\|_1 \right| + \left| \|\tilde{V}\Phi(x-y)\|_1 - \|x-y\|_2 \right| \\ &\leq \|\tilde{V}(Q^{(r)}(\Phi x) - \Phi x) - \tilde{V}(Q^{(r)}(\Phi y) - \Phi y)\|_1 + \left| \|\tilde{V}\Phi(x-y)\|_1 - \|x-y\|_2 \right| \\ &\leq \|\tilde{V}P^r u_x\|_1 + \|\tilde{V}P^r u_y\|_1 + \left| \|\tilde{V}\Phi(x-y)\|_1 - \|x-y\|_2 \right| \\ &\leq \|\tilde{V}P^r\|_{\infty,1}(\|u_x\|_\infty + \|u_y\|_\infty) + \left| \|\tilde{V}\Phi(x-y)\|_1 - \|x-y\|_2 \right| \\ &\leq 2Cc(\mu)^r r^r (8r)^{r+1} \sqrt{\pi/2} \lambda^{-r+1/2} + \epsilon \|x-y\|_2 \\ &= \sqrt{2\pi} Cc(\mu)^r r^r (8r)^{r+1} \lambda^{-r+1/2} + \epsilon \|x-y\|_2 \\ &= C(\mu, r) \lambda^{-r+1/2} + \epsilon \|x-y\|_2 \end{aligned}$$

holds uniformly for any $x, y \in \mathcal{T}$ with probability at least $1 - \delta - 2|\mathcal{T}|e^{-\beta}$. \square

Under the assumptions of Theorem 5.2, we have

$$(28) \quad \epsilon = O\left(\sqrt{\frac{\log(|\mathcal{T}|^2/\delta)}{p}}\right) \lesssim \frac{1}{\sqrt{p}}.$$

By (24), (25) and (28),

$$\begin{aligned} \left| d_{\tilde{V}}(f_i(x), f_i(y)) - \|x-y\|_2 \right| &\leq C(\mu, r) \left(\frac{m}{p}\right)^{-r+1/2} + \epsilon \|x-y\|_2 \\ &\leq C(\mu, r) \left(\frac{m}{p}\right)^{-r+1/2} + 2\kappa\epsilon \\ (29) \quad &\leq C(\mu, r) \left(\frac{m}{p}\right)^{-r+1/2} + \frac{\mu}{\sqrt{\beta + \log(2m)}} \cdot \frac{C_2}{\sqrt{p}} \end{aligned}$$

holds uniformly for any $x, y \in \mathcal{T}$ with high probability. So we can split the reconstruction error into two parts. The first error term in (29) results from $\Sigma\Delta$ quantization while the second error term is caused by CJLT.

It implies that the first term $O((m/p)^{-r+1/2})$ dominates the error when $\lambda = m/p$ is small. If m/p is sufficiently large, the second term $O(1/\sqrt{p})$ will become significant.

6. COMPUTATIONAL & SPACE COMPLEXITY

Suppose that $\mathcal{T} = \{x^{(j)}\}_{j=1}^k \subseteq \mathbb{R}^n$ is a finite dataset. By using HD to flatten $x^{(j)}$ if necessary, without loss of generality we assume that \mathcal{T} consists of well-spread vectors. Moreover, we will focus on stable r -th order $\Sigma\Delta$ schemes $Q^{(r)} : \mathbb{R}^m \rightarrow \mathcal{A}^m$ with $\mathcal{A} = \{-1, 1\}$.

According to Definition 3.3, in the case $r = 1$, we have $v = (1, 1, \dots, 1) \in \mathbb{R}^\lambda$, while when $r = 2$, $v = (1, 2, \dots, \tilde{\lambda} - 1, \tilde{\lambda}, \tilde{\lambda} - 1, \dots, 2, 1) \in \mathbb{R}^\lambda$. In general, one can check that $\|v\|_\infty / \|v\|_2 = O(\lambda^{-1/2})$ holds for all $r \in \mathbb{N}$. So throughout this section we will persist with above setting and assume that $s = \Theta(\epsilon^{-1}n^{-1}(\|v\|_\infty / \|v\|_2)^2) = \Theta(\epsilon^{-1}n^{-1}\lambda^{-1}) \leq 1$ as in Theorem 5.2.

We will consider floating-point or fixed-point representations. Recall that a floating point number is represented approximately to b significant digits/bits (called significand or mantissa) and scaled using an exponent in base 2. Meanwhile, a fixed point number representation has a fixed number of digits after and before the radix point. That is, it has a specific number of bits reserved for the integer part and a specific number of bits reserved for the fractional part. Indeed, the value of a fixed-point number is essentially an integer that is scaled by an implicit specific factor. Suppose that we use b bits and a fixed scaling factor R which is a power of 2 to store fixed point numbers. In both cases we have the same computational complexity for computing sums and products of two numbers. Addition (and subtraction) require $O(b)$ operations while multiplication (and division) can be done in $\mathcal{M}(b) = O(b^2)$ operations using “standard” long multiplication and division. Of course, multiplication and division can be done more efficiently, particularly for large integers. For example, the best known methods (and best possible up to constants) have complexity $\mathcal{M}(b) = O(b \log b)$ [16].

6.1. Embedding Complexity. For each data point $x^{(j)} \in \mathcal{T}$, one can use Algorithm 1 to quantize it. Since A has sparsity constant $s = \Theta(\epsilon^{-1}n^{-1}\lambda^{-1})$ and $\epsilon^{-1} = O(p^{1/2})$ by (28), and since $\lambda = m/p$, computing $Ax^{(j)}$ needs $O(snm) = O(\lambda^{-1}\epsilon^{-1}m) = O(p^{3/2})$ time. Additionally, it takes $O(m)$ time to quantize $Ax^{(j)}$ based on (16). When $p^{3/2} \leq m$, Algorithm 1 can be executed in $O(m)$ for each single data point. Because A has $O(snm) = O(m)$ nonzero entries, the space complexity is $O(m)$ bits per data point. Note that the big O notation here hides the space complexity dependence on the bit-depth b of the fixed or floating point representation of the entries of A and $x^{(j)}$. This clearly has no effect on the storage space needed for each $q^{(j)}$, which is exactly m bits.

6.2. Complexity of Distance Estimation. If one does not use embedding methods, storing \mathcal{T} directly, i.e., by representing the coefficients of each $x^{(j)}$ by b bits requires knb bits. Moreover, the resulting computational complexity of estimating $\|x - y\|_2^2$ where $x, y \in \mathcal{T}$ is $O(n\mathcal{M}(b))$. On the other hand, suppose we obtain binary sequences $\mathcal{B} = \{q^{(j)}\}_{j=1}^k \subseteq \mathcal{A}^m$ by performing Algorithm 1 on \mathcal{T} . Using our method with accuracy guaranteed by Theorem 5.2, high-dimensional data points $\mathcal{T} \subseteq \mathbb{R}^n$ are now transformed into short binary sequences, which only require km bits of storage instead of knb bits. Algorithm 2 can be applied to recover the pairwise ℓ_2 distances. Note that \tilde{V} is the normalization of an integer valued matrix $V = I_p \otimes v$ (by Definition 3.3) and $q^{(i)} \in \mathcal{A}^m$ is a binary vector. So, by storing the normalization factor separately, we can ignore it when considering runtime and space complexity. Thus we observe:

- (1) The number of bits needed to represent each entry of v is at most $\log_2(\|v\|_\infty) \approx (r - 1)\log_2 \lambda = O(\log_2 \lambda)$ when $r > 1$ and $O(1)$ when $r = 1$. So the computation of $y^{(i)} = \tilde{V}q^{(i)} \in \mathbb{R}^p$ only involves m additions or subtractions of integers represented by $O(\log_2 \lambda)$ bits and thus the time complexity in computing $y^{(i)}$ is $O(m \log_2 \lambda)$.
- (2) Each of the p entries of $y^{(i)}$ is the sum of λ terms each bounded by λ^{r-1} . We can store $y^{(i)}$ in $O(p \log_2 \lambda)$ bits.
- (3) Computing $\|y^{(i)} - y^{(j)}\|_1$ needs $O(p \log_2 \lambda)$ time and $O(p \log_2 \lambda)$ bits.

So we use $O(p \log_2 \lambda)$ bits to recover each pairwise distance $\|x^{(i)} - x^{(j)}\|_2$ in $O(m \log_2 \lambda)$ time.

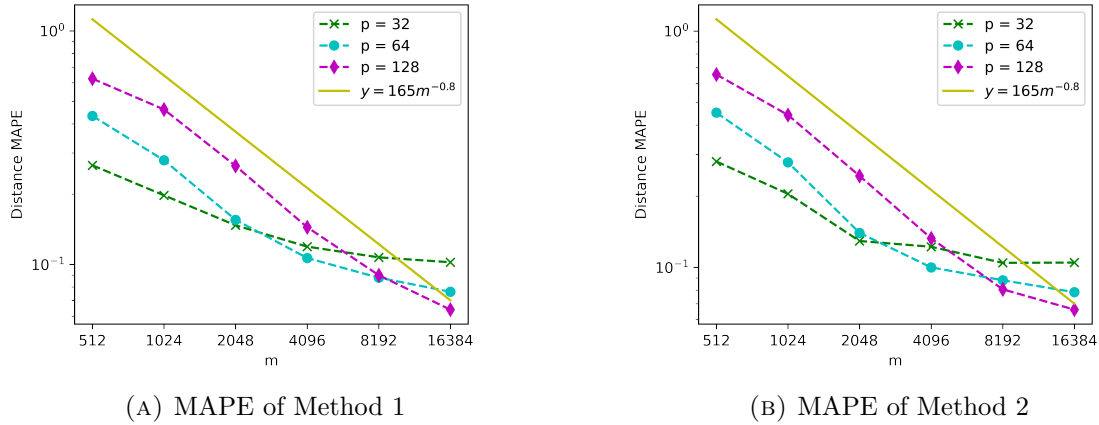


FIGURE 1. Plots of ℓ_2 distance reconstruction error when $r = 1$

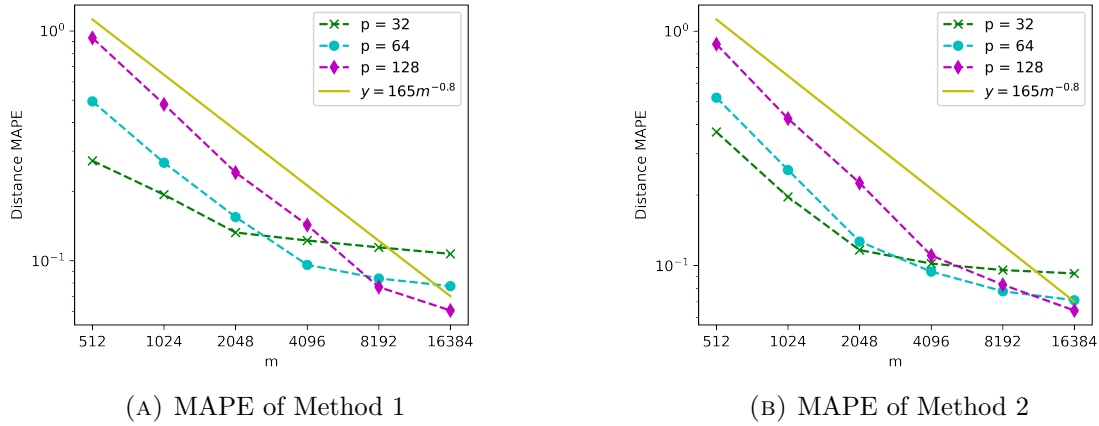


FIGURE 2. Plots of ℓ_2 distance reconstruction error when $r = 2$

7. NUMERICAL EXPERIMENTS

In order to illustrate the performance of fast binary embedding (Algorithm 1) and ℓ_2 norm recovery (Algorithm 2), we will apply these algorithms to a real-world dataset.

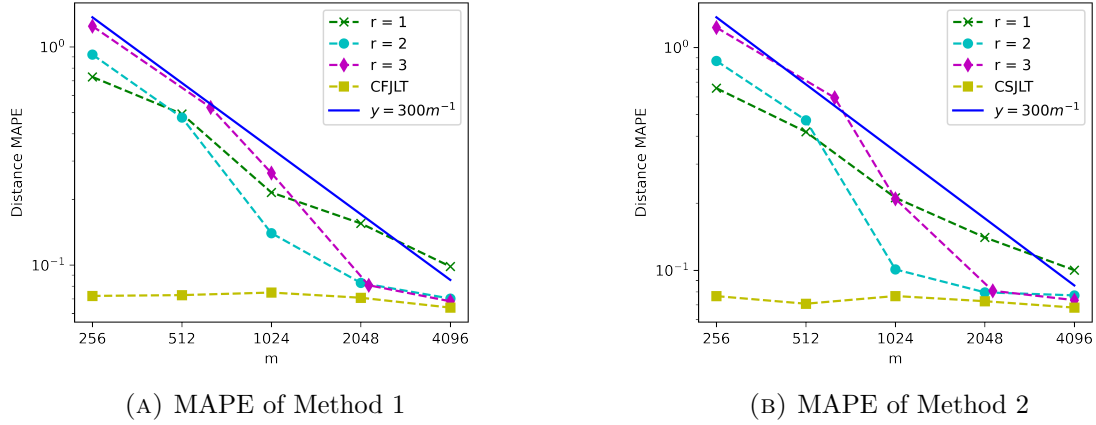
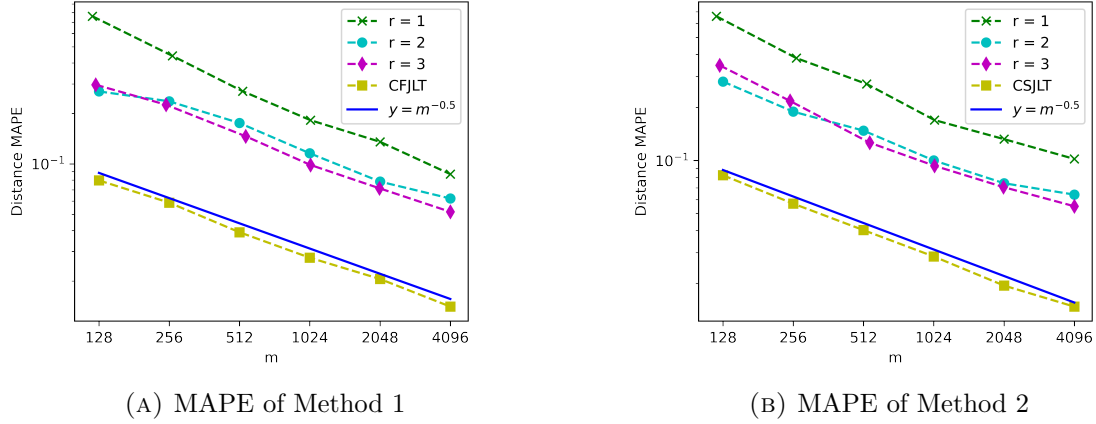
Our dataset comprises $20k$ images provided by Yelp¹ which is a subset of numerous photos of different businesses uploaded by users. Each image is converted to grayscale and resampled using bicubic interpolation on all pixels that may contribute to the output value so that it is resized to 128×128 and can be represented by a 16384 (i.e. 2^{14})-dimensional vector.

We randomly sample $k = 500$ images and scale them by the same constant such that all scaled data points are contained in the ℓ_2 unit ball. The scaled dataset is denoted by \mathcal{T} . Our fast binary embedding algorithm will be performed in two different ways:

Method 1: we quantize the FJLT embeddings, i.e. Φx for $x \in \mathcal{T}$, and reconstruct the ℓ_2 pairwise distances based on Algorithm 2.

Method 2: instead of using FJLT, we quantize the SJLT embeddings Ax and recover distances by Algorithm 2.

¹Yelp open dataset: <https://www.yelp.com/dataset>

FIGURE 3. Plots of ℓ_2 distance reconstruction error with fixed $p = 64$ FIGURE 4. Plots of ℓ_2 distance reconstruction error with optimal $p = p(m)$

In order to test the performance of our algorithm, we will compute the mean absolute percentage error (MAPE) of reconstructed ℓ_2 distances averaged over all pairwise data points, that is,

$$\frac{2}{k(k-1)} \sum_{x,y \in \mathcal{T}} \left| \frac{\|\tilde{V}(q_x - q_y)\|_1 - \|x - y\|_2}{\|x - y\|_2} \right|.$$

Based on Theorem 5.2, we set $n = 16384$ and $s = 1650/n \approx 0.1$. For each fixed p , we implement Algorithm 1 and Algorithm 2 along various m . We present our experimental results for stable $\Sigma\Delta$ quantization schemes, given by (16), with $r = 1$ and $r = 2$ in Figure 1 and Figure 2 respectively. In Figure 1, we observe that the curve with small p quickly reach a flat error while with high p the error decays like $m^{-1/2}$ and eventually reach a lower floor. The reason is that the first error term in (29) is significant especially when m/p is relatively small and the second error term will eventually dominate the total error as m becomes larger and larger. Figure 2 presents similar results but those error curves decay faster than Figure 1 and eventually achieve the same flat error because we use the second order quantizer in this case and the first term in (29) has power $-3/2$ while the second flat error term is independent of r . Moreover, the performance of Method 2 is very similar to that of Method 1.

Next, we illustrate the relationship between the quantization order r and the number of measurements m in Figure 3. The curves obtained directly from an unquantized CFJLT (resp. CSJLT) as in Corollary 3.8, with $m = 256, 512, 1024, 2048, 4096$, and $p = 64$ are used for comparison against the quantization methods. Figure 3 depicts the mean squared relative error when $p = 64$ is fixed for all distinct methods. It shows that stable quantization schemes with order $r > 1$ outperform the first order greedy quantization method, particularly when m is large. Moreover, both the $r = 2$ and $r = 3$ curves converge to the CFJLT/CSJLT result as m goes to 4096. Note that by using a quarter of the original dimension, i.e. $m = 4096$, our construction achieves less than 10% error. Furthermore, if we encode $\tilde{V}q$ as discussed in Section 6.2, then we need at most $rp \log_2 \lambda = 64r \log_2(4096/64) = 384r$ bits per image, which is $\lesssim 0.023$ bits per pixel.

For our final experiment, we illustrate that the error performance of the proposed approach can be further improved. Note that the choice of p only effects the distance computation in Algorithm 2 and does not appear in the embedding algorithm. In other words, one can vary p in Algorithm 2 to improve performance. This can be done either analytically by viewing the right hand side of (29) as a function of p and optimizing for p (up to constants). It can also be done empirically, as we do here. Following this intuition, if we vary p as a function of m , and use the empirically optimal p in the construction of \tilde{V} , then we obtain Figure 4 where the choice $r = 3$ exhibits lower error than other quantization methods. Note that the decay rate, as a function of m , very closely resembles that of the unquantized JL embedding particularly for higher orders r (as one can verify by optimizing the right hand side of (29)).

Acknowledgment. RS and JZ’s work was supported in part by National Science Foundation Grant DMS-2012546 and a UCSD senate research award. The authors would like to thank Sjoerd Dirksen for inspiring discussions and suggestions.

REFERENCES

- [1] N. Ailon and B. Chazelle. The fast johnson–lindenstrauss transform and approximate nearest neighbors. *SIAM Journal on computing*, 39(1):302–322, 2009.
- [2] N. Ailon and E. Liberty. An almost optimal unrestricted fast johnson-lindenstrauss transform. *ACM Transactions on Algorithms (TALG)*, 9(3):1–12, 2013.
- [3] Y. Cheng, X. Y. Felix, R. S. Feris, S. Kumar, A. Choudhary, and S.-F. Chang. Fast neural networks with circulant projections. *arXiv preprint arXiv:1502.03436*, 2, 2015.
- [4] A. Choromanska, K. Choromanski, M. Bojarski, T. Jebara, S. Kumar, and Y. LeCun. Binary embeddings with structured hashed projections. In *International Conference on Machine Learning*, pages 344–353, 2016.
- [5] E. Chou and C. S. Güntürk. Distributed noise-shaping quantization: I. beta duals of finite frames and near-optimal quantization of random measurements. *Constructive Approximation*, 44(1):1–22, 2016.
- [6] I. Daubechies and R. DeVore. Approximating a bandlimited function using very coarsely quantized data: A family of stable sigma-delta modulators of arbitrary order. *Annals of mathematics*, 158(2):679–710, 2003.
- [7] P. Deift, F. Kraher, and C. S. Güntürk. An optimal family of exponentially accurate one-bit sigma-delta quantization schemes. *Communications on Pure and Applied Mathematics*, 64(7):883–919, 2011.
- [8] S. Dirksen and A. Stollenwerk. Fast binary embeddings with gaussian circulant matrices. In *2017 International Conference on Sampling Theory and Applications (SampTA)*, pages 231–235. IEEE, 2017.
- [9] S. Dirksen and A. Stollenwerk. Fast binary embeddings with gaussian circulant matrices: improved bounds. *Discrete & Computational Geometry*, 60(3):599–626, 2018.
- [10] S. Dirksen and A. Stollenwerk. Binarized johnson-lindenstrauss embeddings. *arXiv preprint arXiv:2009.08320*, 2020.
- [11] S. Foucart and H. Rauhut. A mathematical introduction to compressive sensing. *Bull. Am. Math.*, 54:151–165, 2017.
- [12] Y. Gong, S. Kumar, H. A. Rowley, and S. Lazebnik. Learning binary codes for high-dimensional data using bilinear projections. In *Proceedings of the IEEE conference on computer vision and pattern recognition*, pages 484–491, 2013.
- [13] Y. Gong, S. Kumar, V. Verma, and S. Lazebnik. Angular quantization-based binary codes for fast similarity search. In *Advances in neural information processing systems*, pages 1196–1204, 2012.

- [14] Y. Gong, S. Lazebnik, A. Gordo, and F. Perronnin. Iterative quantization: A procrustean approach to learning binary codes for large-scale image retrieval. *IEEE transactions on pattern analysis and machine intelligence*, 35(12):2916–2929, 2012.
- [15] C. S. Güntürk. One-bit sigma-delta quantization with exponential accuracy. *Communications on Pure and Applied Mathematics: A Journal Issued by the Courant Institute of Mathematical Sciences*, 56(11):1608–1630, 2003.
- [16] D. Harvey and J. Van Der Hoeven. Integer multiplication in time $o(n \log n)$. *Preprint*, 2019.
- [17] T. Huynh and R. Saab. Fast binary embeddings and quantized compressed sensing with structured matrices. *Communications on Pure and Applied Mathematics*, 73(1):110–149, 2020.
- [18] L. Jacques, J. N. Laska, P. T. Boufounos, and R. G. Baraniuk. Robust 1-bit compressive sensing via binary stable embeddings of sparse vectors. *IEEE Transactions on Information Theory*, 59(4):2082–2102, 2013.
- [19] W. B. Johnson and J. Lindenstrauss. Extensions of lipschitz mappings into a hilbert space. *Contemporary mathematics*, 26(189-206):1, 1984.
- [20] D. M. Kane and J. Nelson. A derandomized sparse johnson-lindenstrauss transform. *arXiv preprint arXiv:1006.3585*, 2010.
- [21] D. M. Kane and J. Nelson. Sparser johnson-lindenstrauss transforms. *Journal of the ACM (JACM)*, 61(1):1–23, 2014.
- [22] S. Kim, J. Kim, and S. Choi. On the optimal bit complexity of circulant binary embedding. In *AAAI*, pages 3423–3430, 2018.
- [23] F. Krahmer and R. Ward. New and improved johnson–lindenstrauss embeddings via the restricted isometry property. *SIAM Journal on Mathematical Analysis*, 43(3):1269–1281, 2011.
- [24] P. Li, A. Shrivastava, J. L. Moore, and A. C. König. Hashing algorithms for large-scale learning. In *Advances in neural information processing systems*, pages 2672–2680, 2011.
- [25] W. Liu, J. Wang, S. Kumar, and S.-F. Chang. Hashing with graphs. In *ICML*, 2011.
- [26] J. Matoušek. On variants of the johnson–lindenstrauss lemma. *Random Structures & Algorithms*, 33(2):142–156, 2008.
- [27] J. Nelson, E. Price, and M. Wootters. New constructions of rip matrices with fast multiplication and fewer rows. In *Proceedings of the twenty-fifth annual ACM-SIAM symposium on Discrete algorithms*, pages 1515–1528. SIAM, 2014.
- [28] S. Oymak, C. Thrampoulidis, and B. Hassibi. Near-optimal sample complexity bounds for circulant binary embedding. In *2017 IEEE International Conference on Acoustics, Speech and Signal Processing (ICASSP)*, pages 6359–6363. IEEE, 2017.
- [29] Y. Plan and R. Vershynin. Robust 1-bit compressed sensing and sparse logistic regression: A convex programming approach. *IEEE Transactions on Information Theory*, 59(1):482–494, 2012.
- [30] M. Raginsky and S. Lazebnik. Locality-sensitive binary codes from shift-invariant kernels. In *Advances in neural information processing systems*, pages 1509–1517, 2009.
- [31] J. Sánchez and F. Perronnin. High-dimensional signature compression for large-scale image classification. In *CVPR 2011*, pages 1665–1672. IEEE, 2011.
- [32] Y. Xia, K. He, P. Kohli, and J. Sun. Sparse projections for high-dimensional binary codes. In *Proceedings of the IEEE conference on computer vision and pattern recognition*, pages 3332–3339, 2015.
- [33] X. Yi, C. Caramanis, and E. Price. Binary embedding: Fundamental limits and fast algorithm. In *International Conference on Machine Learning*, pages 2162–2170, 2015.
- [34] F. Yu, S. Kumar, Y. Gong, and S.-F. Chang. Circulant binary embedding. In *International conference on machine learning*, pages 946–954, 2014.
- [35] X. Zhang, F. X. Yu, R. Guo, S. Kumar, S. Wang, and S.-F. Chang. Fast orthogonal projection based on kronecker product. In *Proceedings of the IEEE International Conference on Computer Vision*, pages 2929–2937, 2015.

DEPARTMENT OF MATHEMATICS, UNIVERSITY OF CALIFORNIA SAN DIEGO
 Email address: `jiz003@ucsd.edu`

DEPARTMENT OF MATHEMATICS AND HALICIOĞLU DATA SCIENCE INSTITUTE, UNIVERSITY OF CALIFORNIA SAN DIEGO
 Email address: `rsaab@ucsd.edu`